

Nonlinear Schroedinger-Poisson Theory for Quantum-Dot Helium

Gilbert Reinisch^{1,*} and Vidar Gudmundsson^{2,†}

¹Université de Nice - Sophia Antipolis, CNRS, Observatoire de la Côte d'Azur, BP 4229, 06304 - Nice Cédex 4, France

²Science Institute, University of Iceland, Dunhaga 3, IS-107 Reykjavik, Iceland

We use a nonlinear Schroedinger-Poisson equation to describe two interacting electrons with opposite spins confined in a parabolic potential, a quantum dot. We propose an effective form of the Poisson equation taking into account the dimensional mismatch of the two-dimensional electronic system and the three-dimensional electrostatics. The results agree with earlier numerical calculations performed in a large basis of two-body states and provide a simple model for continuous quantum-classical transition with increasing nonlinearity. Specific intriguing properties due to eigenstate non-orthogonality are emphasized.

PACS numbers: 73.21.La, 71.10.Li, 71.90+q

I. INTRODUCTION

Quantum-dots can be viewed as artificially structured atoms in heterojunctions or metal-oxide-semiconductor devices where few electrons are confined to a length comparable to the mesoscopic effective Bohr radius a_B ($a_B \sim 10^{-2} \mu\text{m}$ in the case of GaAs). Though the confinement can *a priori* occur in all three directions, some types of experimentally realized quantum-dots display an extension in the $x - y$ plane which is much larger than in the growth direction z of the underlying semiconductor structure.^{1,2,3} Therefore, these quantum-dots are usually regarded as artificial atoms with a disk-like shape. Since electron numbers N as low as one or two per dot have already been realized,^{1,3} quantum-dot Helium consisting of two electrons trapped in the two-dimensional (2D) axisymmetrical harmonic potential $V(r) = \frac{1}{2}M\omega^2 r^2$, where $r^2 = x^2 + y^2$ and M is the effective electron mass, is actually considered as the simplest realistic model for an interacting quantum system.^{4,5} As itself or amongst other such few-electron systems, it has been extensively studied in the relationship with the development of nanotechnologies.^{6,7,8,9} Both its exact 2D-3D analytical⁸ or 2D numerical⁵ solutions in the presence of a perpendicular homogeneous external magnetic field are known, in particular by use of the separation of the Hamiltonian into its center-of-mass and relative-motion terms, due to the assumption of a parabolic particle confinement. Oscillations between spin-singlet and spin-triplet ground states as a function of the magnetic field strength have been predicted^{2,7} and experimentally observed.³ They are due to the interplay between the dot size and the strength of the magnetic field. Another important competition occurs between the kinetic-energy matrix elements and the electron-electron Coulomb interaction ones when changing the characteristic length L of the quantum dot without changing its shape. Indeed, for small L , the Coulomb interaction becomes negligible and the electrons behave like independent, uncorrelated particles.¹⁰ This happens in particular in the case of strong parabolic confinement $\omega \rightarrow \infty$ since then $L \sim l_0 = \sqrt{\hbar/M\omega} \rightarrow 0$.

In this rich theoretical and experimental context, we wish to emphasize new physical results by use of a quite original – with respect to the above state of the art – differential approach based on the Schroedinger-Poisson (SP) definition of single-particle nonlinear eigenstates in quantum-dot Helium. The problem with such eigenstates is that, being the (stationary) solutions of the SP nonlinear differential system, they are not orthogonal. The whole matrix machinery of quantum mechanics then fails and we are left to return to its *ab-initio* fundamental principles. In particular, the square scalar product $\mathcal{P} = \langle \Psi_a | \Psi_b \rangle^2 \neq 0$ of two such nonlinear eigenstates Ψ_a and Ψ_b defines the probability to find the system in either state when it is known to be in the other one (this probability is of course zero for orthogonal Hilbertian eigenstates). Equivalently – and this will be precisely shown below by use of the Fermi golden rule –, \mathcal{P} yields the transition probability either from Ψ_a to Ψ_b or reverse. Therefore, if Ψ_a is, say, the fundamental eigenstate and Ψ_b is an excited one, \mathcal{P} either measures the probability of an absorption process ($\Psi_a \rightarrow \Psi_b$) or an emission one ($\Psi_b \rightarrow \Psi_a$). The following couple of questions are then addressed and tentative answers provided: i) What energy is actually absorbed or emitted as a consequence of the non-orthogonality of the nonlinear eigenstates $\Psi_{a,b}$? ii) Are the affiliated energy exchanges quantized and how?

The present paper is built as follows. We first display, by use of standard numerical tools,¹¹ the remarkable properties of the solutions $\{u_{\mathcal{N}}, C_{\mathcal{N}}\}$ of the SP dimensionless nonlinear differential system, where \mathcal{N} is the nonlinear control parameter whose value is given by the harmonic trap parabolicity ω . Then we numerically investigate the square scalar product $\mathcal{P}_{13} = \langle u_1 | u_3 \rangle^2 \neq 0$ of its first two (zero-angular-momentum, for the sake of simplicity) eigenstates $u_{1,3}$ when \mathcal{N} is increased. Subscripts always refer, in the present work, to those single-particle energy eigenvalues (in units of $\hbar\omega$) which correspond to the $\mathcal{N} \rightarrow 0$ linear limit. We find an interference-like pattern $\propto \sin^2(\frac{1}{2}\mathcal{N})$. Then we validate the above results both by stressing the link between \mathcal{P}_{13} and Fermi's golden rule for small nonlinearity $\mathcal{N} \leq 1$, as well as by displaying the transition of the system to the asymptotic

semi-classical Thomas-Fermi regime for high values of the nonlinearity $\mathcal{N} \gg 1$. Finally, we test the reliability of the present SP description of quantum-dot Helium by comparison with the existing numerical (Refs (4,5) & (9): respectively Figs 1, 3, and 5) and analytical (Ref. (8): Fig. 1b) data concerning either the fundamental energy level or, like in Ref. (9), its (electro)chemical potential. In all cases our nonlinear SP eigensolutions do agree surprisingly well (i.e. within the percent) with the existing exact results (for comparison, the Hartree and Hartree-Fock departures from the exact PGM fundamental energy eigenvalue⁵ are respectively 44 % and 8 % in PGM's Fig. 3).

Therefore we recover an important property that has already been emphasized in the $N = 2$ Coulomb case, both for atomic Helium¹² and hydrogen ion H^- .¹³ Namely that the SP nonlinear differential description yields surprisingly accurate values for the ground state energy when compared to their corresponding mean-field Hartree-Fock ones. The reason seems to be the very particular physical system that is actually constituted by a mere Cooper-like pair of opposite-spin electrons trapped in the same orbital bound state: one electron, say electron a with orbital wave function Ψ_a , "feels" the repulsive electrostatic potential Φ_b that is being created by its fellow electron b with orbital wave function Ψ_b . This potential Φ_b is defined by the classical Poisson equation $\nabla \cdot \nabla \Phi_b \propto -|\Psi_b|^2$ while Ψ_a is solution of the single-particle Schroedinger equation including both classical potentials, namely the external confining potential $V(r)$ and the electrostatic potential Φ_b . The system is closed by the "bosonic orbital assumption" $\Psi_a \equiv \Psi_b$. As a consequence, there is no (positive) electron self-interaction energy contribution like in Hartree's mean-field description. Neither does (negative) Hartree-Fock's exchange energy play a significant role, due to our $S = 0$ opposite-spin assumption. Therefore, the only remaining difference with respect to the exact corresponding energy eigenvalues might be due – or at least partially – to the next-order (negative) correlation effects.

II. THE 2D RADIAL SCHROEDINGER-POISSON NONLINEAR ORDINARY DIFFERENTIAL SYSTEM

The SP differential system results from coupling the single-particle stationary Schroedinger equation that defines the 2D orbital wave function $\Psi(x, y)$ in the potential $V(x, y) + \Phi(x, y)$

$$\left[-\frac{\hbar^2 \nabla^2}{2M} + V(x, y) + \Phi(x, y) \right] \Psi(x, y) = \mu \Psi(x, y), \quad (1)$$

with the Poisson equation which solely defines the mutual electrostatic repulsive interaction $\Phi(x, y)$ between the two particles^{12,13}

$$\nabla^2 \Phi(x, y) = -2\pi \mathcal{N} \hbar \omega |\Psi(x, y)|^2. \quad (2)$$

Since $|\Psi|^2 \propto [\text{length}]^{-2}$, we must indeed introduce, for dimensional reasons related to Eq. (2), a characteristic energy which we wish to write as $\frac{1}{2} \mathcal{N} \hbar \omega$. The corresponding dimensionless parameter $\mathcal{N} \equiv \mathcal{N}(\omega)$ will be defined below and is a typical measure of the SP nonlinearity. It is important to keep in mind that the above system Eqs (1-2) is only relevant for particles in the same orbital state Ψ .

Assuming the 2D axisymmetrical parabolic confining potential $V(x, y) = V(r) = \frac{1}{2} M \omega^2 r^2$, we have:

$$\Psi(x, y) = \Psi(r, \phi) = \psi(r) e^{im\phi}. \quad (3)$$

The wavefunction Ψ is thus the eigenstate of the angular-momentum operator $-i\hbar \partial / \partial \phi$ related to its eigenvalue $m\hbar$. Its radial part $\psi(r)$, which describes the 2D confinement of the electron system in the $z = 0$ transverse plane with radial symmetry in agreement with the experimental results, is defined by

$$\ddot{u} + \frac{1}{X} \dot{u} + \left[C - \frac{X^2}{4} \right] u = 0; \quad \ddot{C} + \frac{1}{X} \dot{C} + \frac{4m^2}{X^4} = u^2, \quad (4)$$

if we introduce the following dimensionless quantities ($l_0 = \sqrt{\hbar/M\omega}$ is the characteristic parabolic length)

$$X = \sqrt{2} \frac{r}{l_0}; \quad u = \sqrt{\frac{\pi \hbar \mathcal{N}}{M \omega}} \psi; \quad C = \tilde{\mu} - \frac{m^2}{X^2} - \tilde{\Phi}, \quad (5)$$

in order to scale the Poisson nonlinearity (namely, the r.h.s. of Eq. (2)) to unity, as evidenced by the r.h.s. of Eq. (4b). The dot stands for derivation with respect to the (dimensionless) radius X and, as already emphasized, the tilde superscript labels energy in units of $\hbar \omega$. The single-particle probability of presence $|\Psi|^2$ must be normalized to unity. Therefore \mathcal{N} is the corresponding dimensionless norm of the solution u

$$\int |\Psi|^2 d^2 \mathbf{x} = 1 \quad \rightarrow \quad \int_0^\infty u^2 X dX = \mathcal{N}. \quad (6)$$

III. THE NONLINEAR QUANTUM-CLASSICAL TRANSITION

The dimensionless solution of our differential problem Eqs (4) yields $u(r)$ and $C(r)$ as functionals of \mathcal{N} given by Eq. (6). It is defined by the initial conditions $u_0 = u(0)$, $\dot{u}_0 = \dot{u}(0)$, $C_0 = C(0)$ and $\dot{C}_0 = \dot{C}(0)$. Amongst them, u_0 and C_0 are left free and will be chosen by numerical dichotomy, in order to yield regular bound-state eigenstates, i.e. u solutions defined by $u(X) \rightarrow 0$ for $X \rightarrow \infty$ (for practical purposes, it will be sufficient to impose $u(X) < 10^{-7}$ at $X = 9$: see Fig. 2 below). On the other hand, $\dot{C}_0 = 0$ (no potential cusp at $X = 0$) and the determination of the last remaining parameters, namely \dot{u}_0 , proceeds from step-by-step increase of both u_0 and \dot{u}_0 , starting from their linear limit where $u_0 \sim \sqrt{\mathcal{N}} \ll 1$

$$u_0 \ll 1; \quad \dot{u}_0 \sim \dot{u}^{\text{lin}}(0). \quad (7)$$

Here

$$u^{\text{lin}}(X) \propto e^{-\frac{X^2}{4}} X^{\frac{m}{2}} P_n(X), \quad (8)$$

defines⁵ the $\mathcal{N} \rightarrow 0$ linear solutions in terms of the quantum numbers n and m and of the Laguerre polynomial $P_n(X)$, namely $P_0 = 1$; $P_1 = 1 - \frac{1}{2}X^2$; $P_2 = 2 - 2X^2 + \frac{1}{4}X^4$; $P_3 = 6 - 9X^2 + \frac{9}{4}X^4 - \frac{1}{8}X^6$... These single-particle linear parabolic states correspond to the energy eigenvalues

$$E^{\text{lin}} = E_{n,m} = (2n + |m| + 1) \hbar\omega. \quad (9)$$

Figure 1 displays the C_0 versus u_0 spiraling trajectories for the two first $m = 0$ eigenstates u_1 (circles) and u_3 (stars). Recall that the subscripts always refer in the

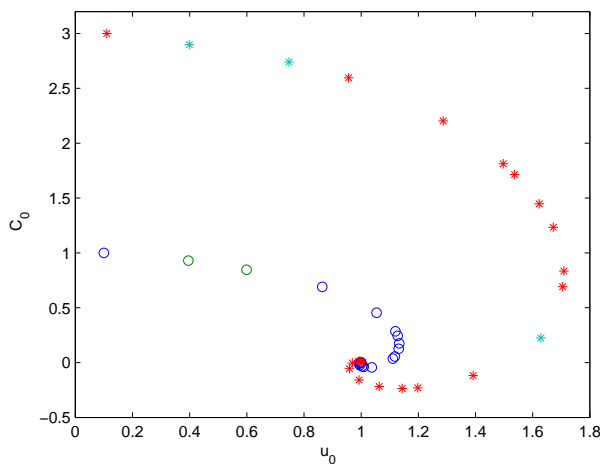


FIG. 1: (Color online). The convergence of the discrete SP nonlinear system towards the quasi-classical continuum Thomas-Fermi regime defined by the fixed point $u \equiv 1$ and $C_0 = \frac{1}{4}[X^2]_{X=0} = 0$ when \mathcal{N} increases from $\sim 10^{-2}$ to $\sim 10^2$ in the $\{C_0 \text{ vs } u_0\}$ boundary condition phase space for the two first $m = 0$ nonlinear eigenmodes defined by their corresponding linear quantum numbers: namely (cf. Eq. (9)) $n = 0, m = 0$ (u_1 : circles) and $n = 1, m = 0$ (u_3 : stars).

present work to the number of $\hbar\omega$ quanta present in the $\mathcal{N} \rightarrow 0$ linear limit of the single-particle energy, in accordance with Eq. 9. These trajectories in the $\{u_0, C_0\}$ plane are parametrized with respect to increasing values of the nonlinear parameter \mathcal{N} , i.e. with decreasing values of the trap harmonic frequency ω . Indeed electron-electron interaction becomes relatively (with respect to quantum kinetic energy) more and more important when the two electrons are less and less confined (see above Part I). Actually \mathcal{N} varies in Fig. 1 from 10^{-2} ($u_0 \sim 0.1$) to 10^2 ($u_0 \sim 1$) where one then reaches the quasi-classical asymptotic Thomas-Fermi regime. This regime is defined by neglecting the quantum kinetic derivative terms in Eq. (4a), thus yielding $C(X) \sim X^2/4$ and hence $C_0 = C(0) = 0$, while $u(X) \equiv 1$ through Eq. (4b). Therefore the initial conditions for the two discrete modes u_1

and u_3 converge towards the Thomas-Fermi fixed point $\{u_0 = 1; C_0 = 0\}$ for $\mathcal{N} \rightarrow \infty$ as evidenced by Fig. 1. Physically, this means that there is a continuous transition, through the increase of nonlinearity in the system, from the $\mathcal{N} \leq \pi$ “pure” quantum regime where the quantum kinetic energy defined by the derivative terms in Eq. (4a) plays a major role towards the $\mathcal{N} \gg \pi$ classical one where the dimensionless Schroedinger equation Eq. (4a) reduces to its last-bracket classical-energy term. As a consequence, the $\mathcal{N} \rightarrow \infty$ highly nonlinear case leads to the progressive merging of the two discrete energy levels u_1 and u_3 into the single one whose initial conditions are defined by the fixed point displayed in Fig. 1. Therefore quantum eigenstate discreteness disappears, which is the hallmark of the classical regime: a continuous energy spectrum sets on about the uniform wavefunction profile $u(X) \equiv 1$ and $C(X) \equiv 0$, where the chemical potential equals the – here vanishing, due to our $m = 0$ assumption – centrifugal potential plus the electrostatic interaction potential, as shown by Eq. (5c).

The onset of the first corresponding oscillation in the amplitude of the respective modes $u_1(X)$ (continuous line) and $u_3(X)$ (dotted line) is displayed in Fig. 2.

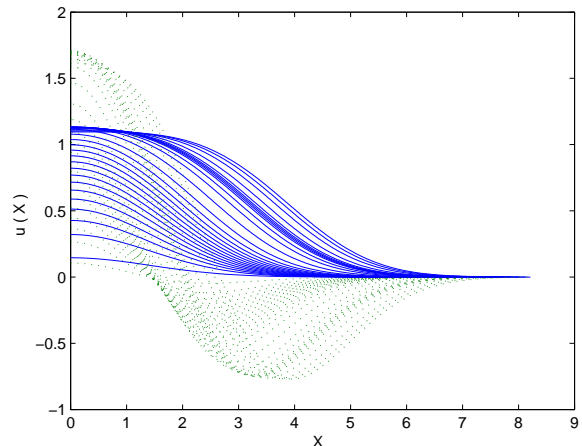


FIG. 2: (Color online). Several nonlinear eigenstate profiles $u_1(X)$ (continuous line) and $u_3(X)$ (dashed line) for increasing values of the dimensionless quantum-dot size k , namely $10^{-2} \leq k \leq 8.7$, where $k = l_0/a^*$ is the ratio of the characteristic harmonic length $l_0 = \sqrt{\hbar/M\omega}$ over the effective Bohr radius $a^* = \hbar^2/Me^2$. The maximum-amplitude thresholds at $u_0 \sim 1.2$ (resp. $u_0 \sim 1.8$) for the ground-state mode u_1 (resp. the excited mode u_3) and displayed by Fig. 1 are clearly visible (profile accumulation effect).

IV. CHEMICAL POTENTIAL AND ENERGY: THE EXPLICIT DEFINITION $\mathcal{N}(\omega)$

In the following, we shall only consider zero-angular-momentum $m = 0$ states for the sake of simplicity (we have indeed checked that $m \neq 0$ nonlinear eigenstates are

equally well described by the above differential system: see below Fig. 4 where the quantum-dot spectra are displayed versus their corresponding \mathcal{N} for $n \leq 3$; $m \leq 3$). The SP virial energy E per particle corresponding to the nonlinear eigenstate $u(X)$ is twice the expectation value $\langle \frac{1}{2} M \omega^2 r^2 \rangle$ of the external parabolic potential energy (virial theorem for a harmonic potential). In terms of the dimensionless quantities defined in Eqs (5), it reads

$$\tilde{E} = \frac{1}{2\mathcal{N}} \int_0^\infty u^2 X^3 dX. \quad (10)$$

On the other hand, the chemical potential μ defined by Eq. (1) is that energy which is required in order to add the second electron to the single-electron quantum-dot (Koopman's theorem¹⁴). It can truly be regarded as the nonlinear eigenvalue of the SP differential system related to the corresponding nonlinear eigenstate Ψ (or u in the reduced units defined in Eqs (5)). Therefore we have

$$\tilde{\mu} = 2\tilde{E} - \tilde{E}^{\text{lin}}, \quad (11)$$

where $E^{\text{lin}} = E_{n,m}$ is defined by Eq. 9. In the present work where we only consider $m = 0$ eigenstates, the two first levels are \tilde{E}_1 (resp. \tilde{E}_3) corresponding to $n = 0$ (resp. $n = 1$) in units of $\hbar\omega$. The nonlinear integrodifferential system Eqs (4-11) is closed by the use of Eq. (5c) at $X = 0$. This yields the (reduced) chemical potential $\tilde{\mu} = \mu/\hbar\omega$ for $m = 0$

$$\begin{aligned} \tilde{\mu} = C(0) + \tilde{\Phi}(0) &= C_0 + \frac{e^2}{\hbar\omega} \int \frac{|\Psi|^2}{r} d^3\mathbf{x} \\ &= C_0 + \frac{\sqrt{2}k}{\mathcal{N}} \int_0^\infty u^2 dX, \end{aligned} \quad (12)$$

where $k = l_0/a^*$ is the usual dimensionless dot size corresponding to the harmonic length $l_0 = \sqrt{\hbar/M\omega}$ and the effective Bohr radius $a^* = \hbar^2/Me^2$ (ranging from $a^* = 67 \text{ nm}$ for InSb to $a^* = 9.8 \text{ nm}$ for GaAs).

Equations (4-12) self-consistently define, for any given value of the trap characteristic harmonic frequency ω (or, equivalently, its reduced size k), the solution $u \equiv u_\omega(X)$, its norm $\mathcal{N} \equiv \mathcal{N}(\omega)$ as well as its corresponding single-particle energy $\tilde{E} \equiv \tilde{E}(\omega)$, together with the chemical potential $\tilde{\mu} \equiv \tilde{\mu}(\omega)$. We numerically obtain, for instance for the ground state in the ‘‘quantum-regime’’ interval of values $\mathcal{N} \leq \pi$ (see below)

$$\mathcal{N}(k) \sim \frac{0.8839 k}{0.4218 + 0.1247 k} \quad (13)$$

while its energy is

$$\tilde{E}(\mathcal{N}) \sim 1 + 0.24670\mathcal{N} + 0.03683\mathcal{N}^2 - 0.00217\mathcal{N}^3. \quad (14)$$

Therefore $\mathcal{N}(k)$ is a monotonic increasing function of the dot size, starting like $\mathcal{N} \sim 2k$ for small values of the dot size k , while

$$\tilde{E} \sim \tilde{E}^{\text{lin}} + \frac{1}{4}\mathcal{N} \quad @ \quad \mathcal{N} < 1 \quad \leftrightarrow \quad k < \frac{1}{2}. \quad (15)$$

In Ref. 5, for instance, where $\hbar\omega = 3.37 \text{ meV}$ for a GaAs parabolic quantum dot (M equals 0.067 electron mass while the charge is $1/\sqrt{12.4}$ electron charge), we have $a^* = 9.79 \text{ nm}$ and $l_0 = 18.5 \text{ nm}$. Hence $k = 1.89$. Then Eqs (13,14) respectively yield $\mathcal{N} = 2.53$ and $\tilde{E} = \tilde{E}_{\text{per particle}} = 1.83$. Therefore $E_{\text{quantum dot}} = 2\tilde{E}_{\text{per particle}} = 2(1.83)\hbar\omega = 12.33 \text{ meV}$ to be compared with PGM's value 12.28 meV: see Fig. 3 where the virial energy per particle (solid line), defined by Eq. (10), is plotted together with the Koopman one (dashed line), defined from Eqs (9-12). The energy per particle \tilde{E} is defined by the intersection of both plots. Similarly, in

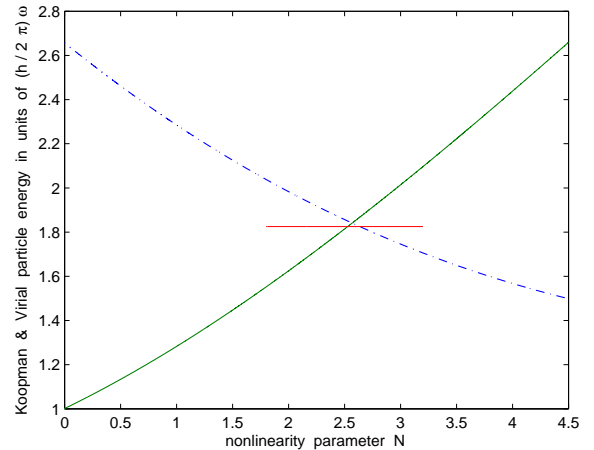


FIG. 3: (Color online). For GaAs quantum-dot Parahelium defined by the confinement $\hbar\omega = 3.37 \text{ meV}$, the dielectric constant of the bulk material $\kappa = 12.4$ and the effective mass $M = 0.067 m_e$ (where m_e is the electron mass),⁵ we have $\mathcal{N} = 2.53$ and $\tilde{E} = 1.831$ by use of (respectively) Eqs (13) & (14). This last SP ground-state energy per particle value appears here as the intersection of its virial (continuous line) and its Koopman (dashed-dotted line) definitions as respectively provided by Eqs (10) & (11-12). PGM's exact numerical value $\tilde{E} = \frac{1}{2}(12.28) \text{ meV} / 3.37 \text{ meV} = 1.822$ given in Ref. (5) is plotted as the horizontal segment.

Ref. 9, $\hbar\omega = 2 \text{ meV}$ yields $k = 2.43$. Hence $\mathcal{N} = 2.97$ and $\tilde{E} = 2.00$, which yields $\tilde{\mu} = 2\tilde{E} - 1 = 3.00$ in accordance with Eq. (11), and therefore $\mu = 3.00\hbar\omega = 6.00 \text{ meV}$ which is in complete agreement with the Coulomb-interaction case ($d_1 = d_2 = \infty$) of that reference.

A remarkable property of the SP nonlinear eigen-solutions is their ‘‘universal’’ limit behavior defined by Eq. (15) for small \mathcal{N} , whatever the actual state's quantum numbers n and m in Eq. (9): see Fig. 4 where $\tilde{E} = \tilde{E}^{\text{lin}} + \frac{1}{4}\mathcal{N}$ is plotted in dashed line. Therefore the energy

$$\Delta = \frac{1}{2}\mathcal{N}\hbar\omega, \quad (16)$$

which was introduced for dimensional reasons into the Poisson equation (2) is simply the smallest additional

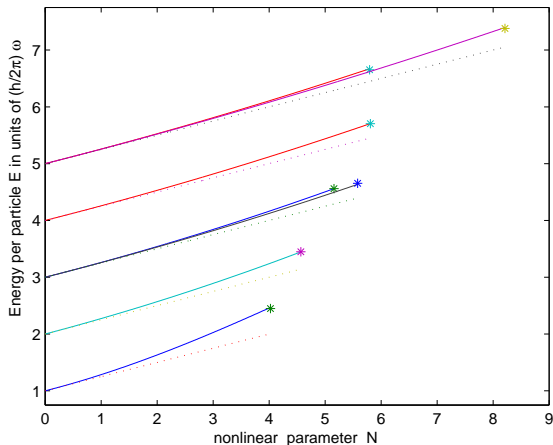


FIG. 4: (Color online). Illustration of Eq. (15) (dotted line) for the $1 \leq \tilde{E}^{\text{lin}} \leq 5$ nonlinear eigenmodes (as defined by their linear $\mathcal{N} \rightarrow 0$ quantum numbers n & m : see Eq. (9)). The stars display the greatest u_0 value reached for each mode: see Fig. 1 for the two first $m = 0$ modes where the stars would respectively correspond to $u_0 \sim 1.2$ and $u_0 \sim 1.7$. From bottom to top (a & b superscripts label degeneracies which are lifted by nonlinearity): $\{n = 0, m = 0\}$, $\{n = 0, m = 1\}$, $\{n = 1, m = 0\}^a$, $\{n = 0, m = 2\}^a$, $\{n = 1, m = 1\}$, $\{n = 2, m = 0\}^b$, $\{n = 1, m = 2\}^b$.

quantum-dot energy due to particle-particle interaction nonlinearity. Indeed Eq. (15) yields for the $2E$ quantum-dot energy

$$\lim_{\mathcal{N} \rightarrow 0} 2E = 2E^{\text{lin}} + \Delta, \quad (17)$$

where E^{lin} is the $\mathcal{N} = 0$ linear energy per particle defined by Eq. (9). Therefore Δ is the smallest interaction (or nonlinear) energy value in our two-electron SP system that comes in addition to the already existing “linear” quanta $\hbar\omega$, when $\mathcal{N} \rightarrow 0$. To see whether Δ is a true “nonlinear quantum” of energy – i.e. whether the energy exchanges between the two levels E_1 and E_3 can be described in the terms of both $\hbar\omega$ and Δ – demands to define the actual transition probability between these levels from the non-orthogonality of the corresponding eigenstates. This will be done in the next part.

V. THE SCALAR PRODUCT $\langle u_1 | u_3 \rangle$ AND THE CORRESPONDING TRANSITION PROBABILITY

Let us define the (normalized) scalar product

$$\langle u_1 | u_3 \rangle = \frac{1}{\sqrt{\mathcal{N}_1 \mathcal{N}_3}} \int_0^\infty u_1 u_3 X dX, \quad (18)$$

together with

$$\frac{\int_0^\infty u_1^2 X^3 dX - \mathcal{N}_1 (1 + C_0^{(1)})}{\int_0^\infty u_3^2 X^3 dX - \mathcal{N}_3 (3 + C_0^{(3)})} = \frac{\int_0^\infty u_1^2 dX}{\int_0^\infty u_3^2 dX}, \quad (19)$$

of both zero-angular-momentum eigenstates $u_1(X)$ and $u_3(X)$ corresponding to those energies E_1 and E_3 which are respectively defined at $\mathcal{N}_{1,3} \rightarrow 0$ by $E_{0,0}$ and $E_{1,0}$ in Eq. (9). Equation (19) is the matching condition

$$k(\omega) = \frac{\mathcal{N}_1 (\tilde{\mu}_1 - C_0^{(1)})}{\sqrt{2} \int_0^\infty u_1^2 dX} = \frac{\mathcal{N}_3 (\tilde{\mu}_3 - C_0^{(3)})}{\sqrt{2} \int_0^\infty u_3^2 dX}, \quad (20)$$

defined by Eqs (7-12) which states that the trap harmonicity ω , or equivalently its quantum-dot dimensionless length $k = \sqrt{\hbar/M\omega}/(\hbar^2/Me^2)$, must be identical for the two modes $u_{1,3}$ that enter the calculation of the scalar product (18). Practically, in the numerical simulations of Eqs (18-20), we will consider Eq. (19) as verified if it is fulfilled within an 10^{-6} error.

In order for the scalar product Eqs (18-20) to make physical sense, we wish to link it with standard time-independent linear perturbation theory in the case of small nonlinearity $\mathcal{N} \ll 1$, i.e. for small “perturbative” particle-particle interaction Φ defined by Eqs (1-2). Therefore we deduct that

$$\lim_{\mathcal{N} \rightarrow 0} \langle u_1 | u_3 \rangle^2 = \mathcal{P}_{13}, \quad (21)$$

where

$$\mathcal{P}_{13} = \frac{4}{\hbar^2} |\langle u_3^{\text{lin}} | H^{\text{pert}} | u_1^{\text{lin}} \rangle|^2 \frac{\sin^2(\frac{1}{2}\omega_{13}t)}{\omega_{13}^2}, \quad (22)$$

together with $\hbar\omega_{13} = E_3 - E_1 \sim 2\hbar\omega$, yields Fermi golden rule’s transition probability per particle.¹⁵ Indeed both the energies $E_i \sim E_{\frac{1}{2}(i-1),0}$ per particle ($i = 1, 3$: cf. Eq. (9)) and the corresponding normalized eigenstates $u_i \sim u_i^{\text{lin}}$ in Eq. (22) are those corresponding to the unperturbed linear system (hence the superscript), namely⁵ $u_1^{\text{lin}} = e^{-X^2/4}$ and $u_3^{\text{lin}} = (1 - \frac{X^2}{2})e^{-X^2/4}$ (cf. Eqs (8)). The perturbation potential \tilde{H}^{pert} is equal to $\frac{1}{2}\tilde{\Phi}$ (per particle: hence the factor $\frac{1}{2}$) where $\tilde{\Phi} = \frac{1}{2}[\tilde{\Phi}^{(1)} + \tilde{\Phi}^{(3)}]$ is the interaction potential that has been averaged over its two components $\tilde{\Phi}^{(1)}$ and $\tilde{\Phi}^{(3)}$. Therefore

$$\begin{aligned} \langle u_3^{\text{lin}} | \tilde{H}^{\text{pert}} | u_1^{\text{lin}} \rangle &= \tilde{H}_{13}^{\text{pert}} = \frac{1}{2} [\tilde{\Phi}_{13}] \\ &= \frac{1}{4} [\tilde{\Phi}_{13}^{(1)} + \tilde{\Phi}_{13}^{(3)}], \end{aligned} \quad (23)$$

where the matrix elements $\tilde{\Phi}_{13}^{(i)}$ ($i = 1, 3$) have been calculated by use of the above-mentioned linear normalized eigenstates $u_{1,3}^{\text{lin}}$. In the stationary perturbative regime where $\omega_{13}t \sim 2\omega t \gg 1 \gg H^{\text{pert}}t/\hbar$, the time-dependent

term in Eq. (22) can be replaced by its averaged value $\frac{1}{2}$, yielding $\mathcal{P}_{13} = \frac{1}{2} [\tilde{H}_{13}^{\text{pert}}]^2 = \frac{1}{32} [\tilde{\Phi}_{13}^{(1)} + \tilde{\Phi}_{13}^{(3)}]^2$. Therefore Eq. (21) becomes

$$\lim_{\mathcal{N} \rightarrow 0} \bar{\Phi}_{13} = \frac{1}{2} \lim_{\mathcal{N} \rightarrow 0} [\tilde{\Phi}_{13}^{(1)} + \tilde{\Phi}_{13}^{(3)}] = 2\sqrt{2} |\langle u_1 | u_3 \rangle|. \quad (24)$$

Figure 5 displays the r.h.s. of Eq. (24) (continuous line) versus its l.h.s. (dashed-dotted line) and shows the numerical fulfilment of this condition.

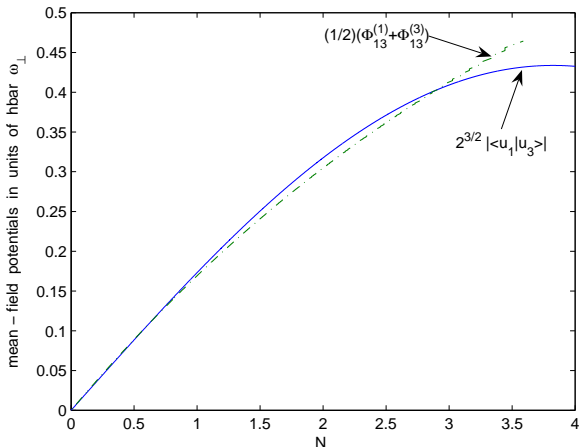


FIG. 5: (Color online). the convergence for small nonlinearity $\mathcal{N} \sim \mathcal{N}_1 \sim \mathcal{N}_3 < 1$ of the SP nonlinear model towards Fermi's "golden rule" probability transition defined by Eqs (18-22), as displayed by Eq. (24).

Therefore the square scalar product defined by Eqs (18-20) yields, in the limit of small nonlinearity $\mathcal{N}_{1,3}$, the transition probability \mathcal{P}_{13} from the fundamental nonlinear eigenstate u_1 to the excited one u_3 or reverse. On the other hand, we showed in Section III that the quasi-classical Thomas-Fermi regime yields $\lim_{\mathcal{N} \rightarrow \infty} u_{1,3} \equiv 1$ (see Fig. 1). The two modes $u_{1,3}$ then become equivalent. Consequently the transition probability between them should obviously become equal to unity, which is consistent with $[\langle u_1 | u_3 \rangle^2]_{u_1 \sim u_3} = 1$ from definition (18). Therefore it seems quite natural to extrapolate to all values of the nonlinearity $\mathcal{N}_{1,3}$ the physical meaning of $\langle u_1 | u_3 \rangle^2$ in terms of the transition probability \mathcal{P}_{13} as defined by Eqs (21-22).

VI. QUANTUM TRANSITIONS BETWEEN TWO $m = 0$ NONLINEAR EIGENSTATES

Let us now proceed to the investigation of the quantum transitions between the two nonlinear eigenstates $u_{1,3}$ by use of the numerical calculation of the scalar product defined by Eqs (18-20). It consists in increasing the nonlinearity through a three-loop iterative scheme from the $\mathcal{N} \ll 1$ linear regime. The two first loops define each eigenstate $u_{1,3}$ which vanish with a 10^{-7} accuracy at

$X \sim 9$ which is our numerical value for $X \sim \infty$ (see Fig. 2) while the third one evaluates the matching condition Eq. (19) within 10^{-6} and then calculates the scalar product given by Eq. (18). The integrals which appear in Eqs (18-20) are transformed into additional first-order ordinary differential equations with vanishing initial conditions whose solutions are taken at $X \sim 9$. Then the whole resulting differential system is numerically integrated by use of standard tools.¹¹

Figure 6 displays the following remarkable interference-like pattern with respect to the ground-state nonlinear parameter \mathcal{N}_1 . Intriguing enough, since the present SP

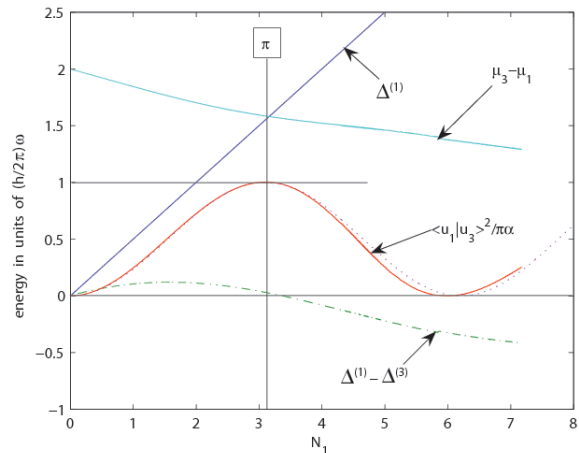


FIG. 6: (Color online). Equation (25)'s square scalar product $\langle u_1 | u_3 \rangle^2 / \pi\alpha$ normalized by $\pi\alpha = \pi/137.036$, as compared with its \sin^2 approximation (dotted line), together with the nonlinear resonance condition Eq. (26) (in "tilde" units of $\hbar\omega$): i) intersection of the two upper plots that yields $\tilde{\mu}_3 - \tilde{\mu}_1 \sim \tilde{\Delta}_1 \sim \pi/2$, and ii) intersection of the dashed-dotted lower plot with zero that yields $\tilde{\Delta}_1 \sim \tilde{\Delta}_3$, i.e. $\mathcal{N}_1 \sim \mathcal{N}_3$, at the resonance nonlinearity $\mathcal{N}_1 \sim \pi$.

differential model is non-relativistic (there is no velocity of light in it), it is best scaled by use of the numerical value of the fine-structure-constant $\alpha = e^2/\hbar c$ multiplied by π , namely $\pi/137.036 = 2.2925... \cdot 10^{-2}$

$$\frac{1}{\pi\alpha} \langle u_1 | u_3 \rangle^2 \sim 1.0005 \sin^2 [0.5060 \mathcal{N}_1]. \quad (25)$$

We note that, when $\mathcal{N}_1 > 4$, the departure from the r.h.s. of Eq. (25) (dotted line in Fig. 6) becomes significant as the transition toward the asymptotic quasi-classical Thomas-Fermi regime sets on. On the other hand, Fig. 6 displays the following chemical-potential gap transition process

$$\mu_3 - \mu_1 \sim \Delta_\pi, \quad (26)$$

where $\Delta_\pi \sim \Delta_1 \sim \Delta_3 \sim \frac{\pi}{2} \hbar\omega_\pi$ is the common characteristic energy Δ , defined by Eq. (16), of the two eigenstates $u_{1,3}$ about the maximum (of amplitude $1.0005 \pi\alpha$)

of their square scalar product $\langle u_1|u_3\rangle^2$, i.e. at the very peculiar quantum-dot nonlinearity $\mathcal{N}_1 \sim \mathcal{N}_3 \sim \pi$ related to the particular $\omega = \omega_\pi$ trap parabolicity. This value corresponds to the specific parabolic confinement $\hbar\omega_\pi \sim 0.14\epsilon$ where $\epsilon = Me^4/\hbar^2$ is the effective quantum-dot's atomic energy unit: $\epsilon = 11.86$ meV for AsGa, thus yielding $\hbar\omega_\pi \sim 1.66$ meV and $\Delta_\pi \sim 2.61$ meV while $\epsilon = 27.21$ eV if the dielectric constant of the bulk material equals unity, then yielding $\hbar\omega_\pi \sim 3.80$ eV and therefore $\Delta_\pi \sim 5.97$ eV. According to Eq. (11), Eq. (26) yields the corresponding quantization rule for the $2E$ quantum-dot energy at $\omega \sim \omega_\pi$

$$2(E_3 - E_1) \sim 2\hbar\omega_\pi + \Delta_\pi. \quad (27)$$

Equations (17) and (27) show that the characteristic energy Δ which scales the electrostatic particle-particle interaction through the nonlinear differential Poisson equation (2) is in fact a true “nonlinear quantum”. Indeed, on the one hand, it is the smallest particle-particle interaction energy present in the system at vanishing nonlinearity $\mathcal{N} \rightarrow 0$. On the other hand, the maximum of the $\langle u_1|u_3\rangle^2$ transition probability between the two states is reached at resonance, i.e. either when Δ equals their nonlinear-eigenvalue chemical-potential gap or when their quantum-dot energy gap is but the mere sum of the two standard “linear” radial quanta $\hbar\omega$ and Δ .

VII. CONCLUSION AND PERSPECTIVES

In the present paper, we have described the parabolic quantum dot by use of the nonlinear differential eigenproblem Eqs (1-2) and emphasized its relevance with respect to all existing corresponding results in the literature. This Schroedinger-Poisson (SP) differential system yields new quantum concepts such as the non-orthogonal nonlinear eigenstates Ψ and their corresponding chemical-potential nonlinear eigenvalues μ .¹⁶ In order to comply with the dimensional self-consistence between the two-dimensional electronic system and its three-dimensional electrostatics, we scaled the Poisson equation according to the characteristic energy $\Delta = \frac{1}{2}\mathcal{N}\hbar\omega$ where \mathcal{N} is a normalized (see Eq. (6)) measure of the system nonlinearity. We showed that Δ is actu-

ally the true “nonlinear energy quantum” of the system for: i) it is the smallest additional “nonlinear” particle-particle interaction energy with respect to the standard “linear” radial harmonic quantum $\hbar\omega$ when $\mathcal{N} \rightarrow 0$ (see Eq. (17)); ii) it fits with that nonlinear-eigenvalue (or chemical-potential) gap between the two first zero-angular-momentum eigenstates which occurs about the maximum of their square scalar product $\langle u_1|u_3\rangle^2$ (see Eqs (26-27)), i.e. about the maximum of their transition probability \mathcal{P} (as a consequence of Fermi's golden rule).

Further developments of the present work should (non exhaustively) address the two following experimental, numerical as well as theoretical topics:

1) Could the nonlinear resonance defined by Eqs (26-27) at the very particular trap parabolicity $\hbar\omega = \hbar\omega_\pi$ (= 1.66 meV for GaAS) be observable and how? It would be a definite plus for the present model to provide an opportunity for experimental verification.

2) The $\pi\alpha$ scaling adopted in Eq. (25) seems extremely accurate. Indeed the square scalar product maximum divided by π approaches the numerical value $1/137.036$ of the fine-structure-constant $e^2/\hbar c$ within 0.05 % in the latest state of our numerical simulations

$$\frac{1}{\pi}\langle u_1|u_3\rangle_{max}^2 = \frac{1}{136.97}. \quad (28)$$

It seems hard to believe that Eq. (28) is but the result of a mere numerical coincidence. Rather, we wish to point out that Eq. (28) might echo Feynman's emphasis of such a “magic number”.¹⁷ This stunning non-relativistic property of the nonlinear-eigenstate square-scalar-product scaling will be further investigated in a future publication.

Acknowledgments

The authors acknowledge financial support from the Research and Instruments Funds of the Icelandic State, the Research Fund of the University of Iceland. One of the authors (GR) feels indebted to P. Valiron for sharp criticisms and very useful discussions and comments. He thanks J. Bec for double-checking the numerical procedures.

* Electronic address: Gilbert.Reinisch@oca.eu

† Electronic address: vidar@raunvis.hi.is

¹ C. Sikorski and U. Merkt, Phys. Rev. Lett **62**, 2164 (1989).

² P. A. Maksym and T. Chakraborty, Phys. Rev. Lett **65**, 108 (1990).

³ R. C. Ashoori, H. L. Stormer, J. S. Weiner, L. N. Pfeiffer, K. W. Baldwin, and K. W. West, Phys. Rev. Lett. **71**, 613 (1993).

⁴ U. Merkt, J. Huser, and M. Wagner, Phys. Rev. B **43**, 7320

(1991).

⁵ D. Pfannkuche, V. Gudmundsson, and P. Maksym, Phys. Rev. B **47**, 2244 (1993).

⁶ P. A. Maksym, Phys. Rev. B **53**, 10871 (1996).

⁷ M. Wagner, U. Merkt, and A. Chaplik, Phys. Rev. B **45**, 1951 (1992).

⁸ M. Dineykh and R. G. Nazmitdinov, Phys. Rev. B **55**, 13707 (1997).

⁹ L. D. Hallam, J. Weis, and P. A. Maksym, Phys. Rev. B

- 53**, 1452 (1996).
- ¹⁰ G. W. Bryant, Phys. Rev. Lett. **59**, 1140 (1987).
- ¹¹ The MathWorks, Inc. (2004), MATLAB, Version 7.0.1.24704 (R14), options = odeset('RelTol',1e-10).
- ¹² G. Reinisch, J. de Freitas Pacheco, and P. Valiron, Phys. Rev. A **63**, 042505 (2001).
- ¹³ G. Reinisch, Phys. Rev. A **70**, 033613 (2004).
- ¹⁴ A. Szabo and N. S. Ostlund, *Modern Quantum Chemistry: Introduction to Advanced Electronic Structure Theory* (Dover, New York, 1996).
- ¹⁵ R. P. Feynman and A. R. Hibbs, *Quantum Mechanics and Path Integrals* (McGraw-Hill Book Company, 1965).
- ¹⁶ G. Reinisch, Physical Review Letters **99**, 120402, (2007).
- ¹⁷ [The numerical value $\sim 1/137$ of the fine-structure-constant $\alpha = e^2/\hbar c$] ... "has been a mystery ever since it was discovered... It's one of the *greatest* damn mysteries of physics: a *magic number* that comes to us with no understanding by man ... We know what kind of a dance to do experimentally to measure this number very accurately, but we don't know what kind of a dance to do on a computer to make this number come out —without putting it in secretly!", in R. P. Feynman, *QED: the strange theory of light and matter*, University Press, (1985).